

REPORT

Title Increasing Water Security through Horizontal Wells

Project Number 2014TX469B

Primary PI Dr. Hongbin Zhan

Other PIs Benjamin Blumenthal

Abstract

Groundwater wells can have extreme pressure buildup when injecting and extreme pressure drawdown when extracting. Greater wellbore contact with the aquifer minimizes pressure buildup and pressure drawdown. Aquifers are usually much more laterally extensive than vertically thick. Therefore, horizontal wells can be longer than vertical wells thus increasing aquifer contact and minimizing pressure issues. The length and therefore the effectiveness of horizontal wells are limited by two factors, either well construction or intra-wellbore head loss.

Currently no analytical groundwater model rigorously accounts for intra-wellbore kinetic and/or friction head loss. We have developed a semi-analytical, intra-wellbore head loss model dynamically linked to an aquifer. This model is the first of its kind in the groundwater literature. We also derived several new boundary condition solutions that are rapidly convergent at all times. These new aquifer solutions do not require approximation or pressure pulse tracking.

We verified our intra-wellbore head loss model against MODFLOW-CFP and found matches of three significant figures. We then completed 360 simulations to investigate intra-wellbore head loss. We found that only when aquifer drawdown was small will intra-wellbore head loss be relatively important. We found intra-wellbore head loss is relatively important only in extreme scenarios. We also found that kinematic head loss was greater than friction head loss if the well was less than 10m – 100m long.

To investigate well construction limitations, we developed an equation for the optimal slant rig entry angle, a drilling forces model, and a well construction cost model. We then collected well cost data and combined these models to make 60 well cost estimates. We found the relative cost of a horizontal well, compared to a vertical well, decreases with depth.

We then used our aquifer model to investigate the benefits of horizontal wells. We found several parameters that increase the number of vertical wells replaced by a horizontal well. These

parameters include less time since pumping began, nearby recharge boundaries, vertical fractures, lower permeability, higher specific storativity, and thinner aquifers. Comparing horizontal well benefit with cost, we found that horizontal wells may or may not be economically advantageous depending on site specific conditions.

Problem and Research Objectives

Groundwater wells (including aquifer storage and recovery wells) can have extreme pressure buildup when injecting and extreme pressure drawdown when extracting. Greater wellbore contact with the aquifer minimizes pressure buildup and pressure drawdown. Aquifers are usually much more laterally extensive than vertically thick. Therefore, horizontal wells can be longer than vertical wells thus increasing aquifer contact and minimizing pressure issues (Figure 1). The length and therefore the effectiveness of horizontal wells are limited by two factors, either well construction (physical and economic limitations) or intra-wellbore head loss.

While current finite-difference models can model intra-wellbore head loss (MODFLOW-CFP), finding a stable solution is a labor intensive process. An analytical model is preferred as these models are easier to use and do not have mass balance or stability issues. Currently no analytical groundwater model rigorously accounts for intra-wellbore kinetic and friction head loss (Hantush and Papadopoulos, 1962; Park and Zhan, 2002; Williams, 2013; Zhan et al, 2001; Zhan and Zlotnik, 2002). Furthermore, previous analytical solutions for horizontal wells are slowly convergent at early times (Goode, 1987; Odeh and Babu, 1990; Park and Zhan, 2002; Zhan et al, 2001). These previous solutions typically require pressure pulse tracking and approximation at early time in addition to restrictions on wellbore location.

To determine the limitations of horizontal well construction, the calculation of drilling geometry, forces, and associated cost is necessary. Currently there is no directional drilling forces model in the groundwater literature. There has also been no discussion of optimal slant rig entry angle in either groundwater or petroleum literature. There has also been very limited discussion of horizontal well cost in the groundwater or petroleum literature (Jehn-Dellaport, 2004; Joshi, 2003).

To address these horizontal groundwater well research needs, we first derive new analytical drawdown/discharge solutions that are rapidly convergent at all times. We then use these new solutions to develop a well model accounting for intra-wellbore kinetic and friction

head loss. Next we develop a drilling forces model which calculates required rig torque, thrust, and pullback along with casing strengths. We also derive the optimal slant rig entry angle to minimize the length of the wellbore and therefore minimize cost. A well cost model is also developed and cost input data gathered. Finally, a horizontal well cost-benefit analysis is completed.

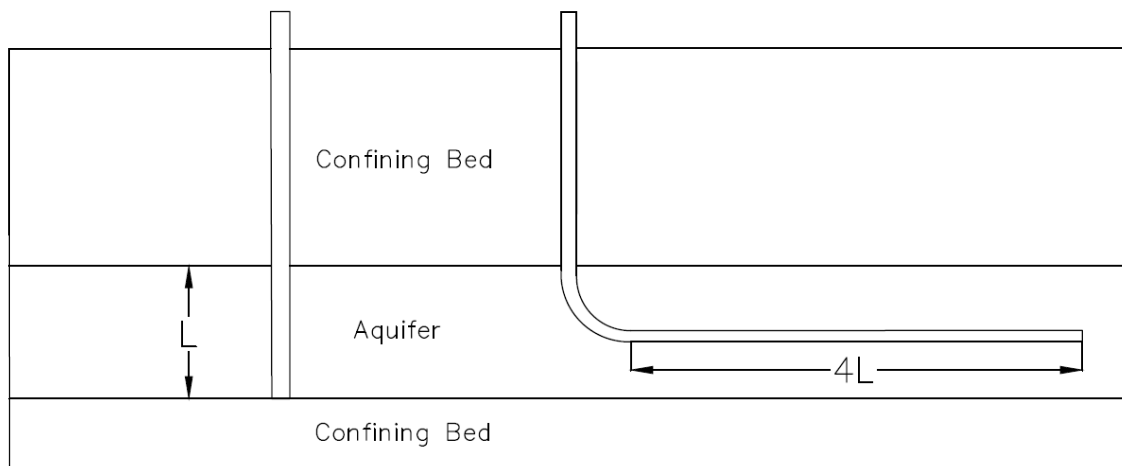


Figure 1. Horizontal wells can facilitate greater contact with the aquifer than vertical wells.

Methods

New Aquifer Solutions

The mathematical relationship between a well's pumping rate and aquifer drawdown begins with the derivation of a point source / sink. This point source / sink has a pumping rate $Q(t)$ [L^3T^{-1}] that is positive for extraction (sink) and negative for injection (source). The point source / sink may be located anywhere inside a box. The dimensions [L] of the box are a , b , c for the x -axis, y -axis and z -axis respectively. The point source / sink is located at x_0 , y_0 , z_0 [L]. The point source / sink affects drawdown at some point x , y , z [L] (Figure 2).

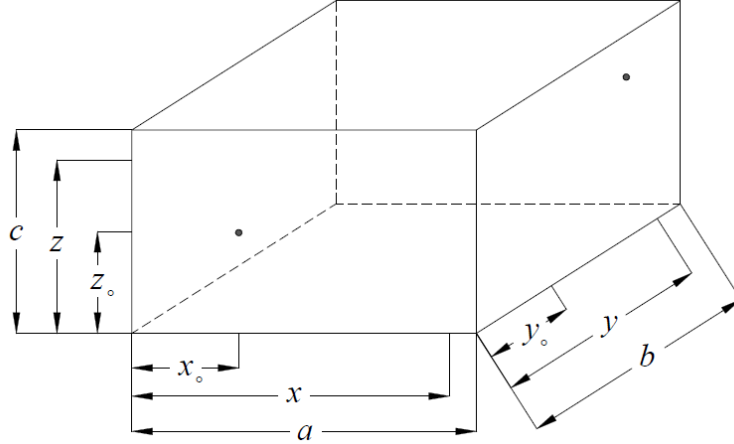


Figure 2. Aquifer conceptual model with source / sink and sample point.

Derivation of our analytical solutions begins with the partial differential equation governing confined groundwater flow

$$S_s \frac{\partial h}{\partial t} = K_x \frac{\partial^2 h}{\partial x^2} + K_y \frac{\partial^2 h}{\partial y^2} + K_z \frac{\partial^2 h}{\partial z^2} - Q(t) \delta(x - x_0) \delta(y - y_0) \delta(z - z_0),$$

where S_s is specific storage [L^{-1}], h is head [L], t is time [T], K_x , K_y , K_z are hydraulic conductivities [LT^{-1}], $Q(t)$ [L^3T^{-1}] is the pumping rate (positive for extraction) as a function of time, and δ is the Dirac delta function (point sink).

We then compute the time Laplace transform to remove time dependence. There are three possible boundary conditions for each of the six sides of the box shaped reservoir. The boundary of any one side of the box may be constant head, no flux, or non-existent. We first solve the boundary value problem (BVP) in the Laplace domain using the method of undetermined coefficients, and then take the inverse Laplace transform to yield solutions in the real time domain.

We now have a solution for a point sink that is slowly convergent at early time. To improve early time convergence, we conduct the Poisson Re-Summation for each of the boundary condition solutions (Strikwerda, 2004). We then derive the time at which the two solutions convergence rates are equal (11 iterations until convergence) and then install a switch between the two methods. We now have a set of solutions that are rapidly convergent (less than 11 iterations) at all times. We then parameterize the solution and use an integral averaging procedure to transform the point sink into a well with three-dimensional length and radius.

Intra-Wellbore Head Loss

We have developed a semi-analytical, intra-wellbore head loss model dynamically linked to a confined aquifer based on petroleum engineering methods (Ouyang et al. 1998; Penmatcha and Aziz, 1999). This method discretizes the well into several uniform flux segments (Figure 3). Using the principal of superposition, we connect these segments. We have setup the equation to solve for d , the drawdown distribution, which is calculated upon multiplication of F (the aquifer response to pumping) with the pumping rate distribution, $FQ = d$.



Figure 3. Wellbore subdivided into four segments.

With the segments linked, we then define the difference in drawdown (head loss) between each segment. This drawdown difference may be either zero (infinite conductivity), depend on friction (frictional head loss) and/or depend on velocity (kinetic head loss). The solution assuming a pumping rate constraint is

$$\begin{pmatrix} F_{1,1} - F_{2,1} & F_{1,2} - F_{2,2} & F_{1,3} - F_{2,3} & F_{1,4} - F_{2,4} \\ F_{2,1} - F_{3,1} & F_{2,2} - F_{3,2} & F_{2,3} - F_{3,3} & F_{2,4} - F_{3,4} \\ F_{3,1} - F_{4,1} & F_{3,2} - F_{4,2} & F_{3,3} - F_{4,3} & F_{3,4} - F_{4,4} \\ 1 & 1 & 1 & 1 \end{pmatrix} \begin{pmatrix} Q_1 \\ Q_2 \\ Q_3 \\ Q_4 \end{pmatrix} = \begin{pmatrix} d_1 - d_2 \\ d_2 - d_3 \\ d_3 - d_4 \\ Q_{Total} \end{pmatrix},$$

where $F_{1,2}$ is how segment two affects segment one, Q_1, Q_2 , etc. is the pumping rate at a specific segment, Q_{Total} is the total pumping rate of the well, and d_1, d_2 , etc. is the drawdown at a specific segment. To verify the accuracy of our intra-wellbore head loss model, we compared it to MODFLOW-CFP and found matches of three significant figures for both steady state (Figure 4 & 5) and transient simulations (Figure 6 & 7).

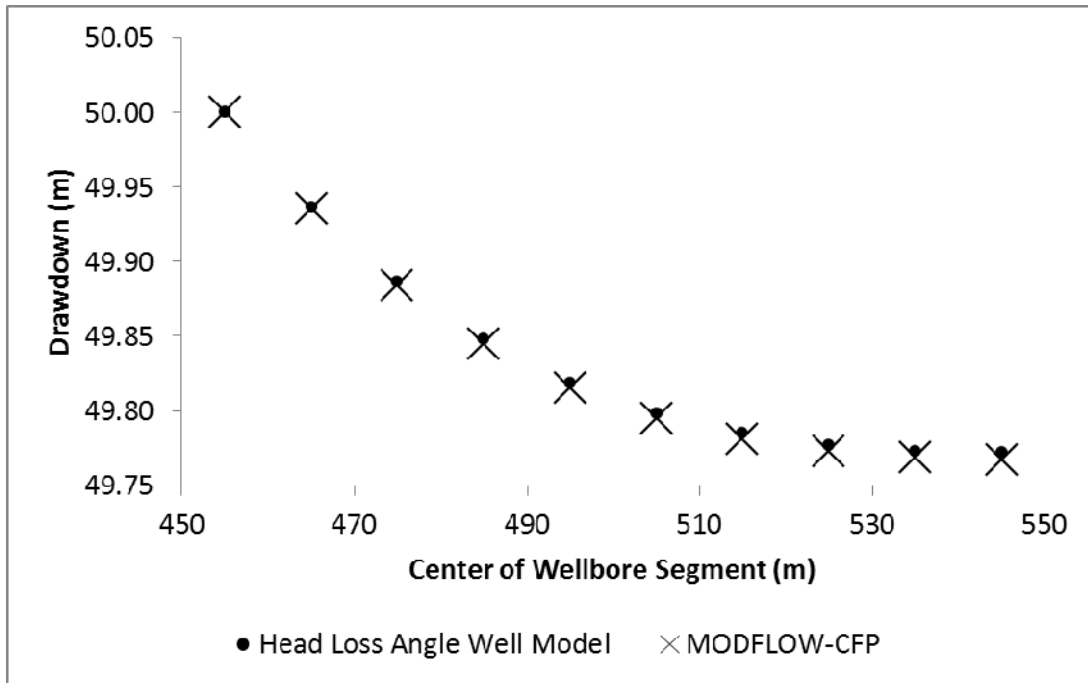


Figure 4. Steady state drawdown distribution verification between our model and MODFLOW-CFP.

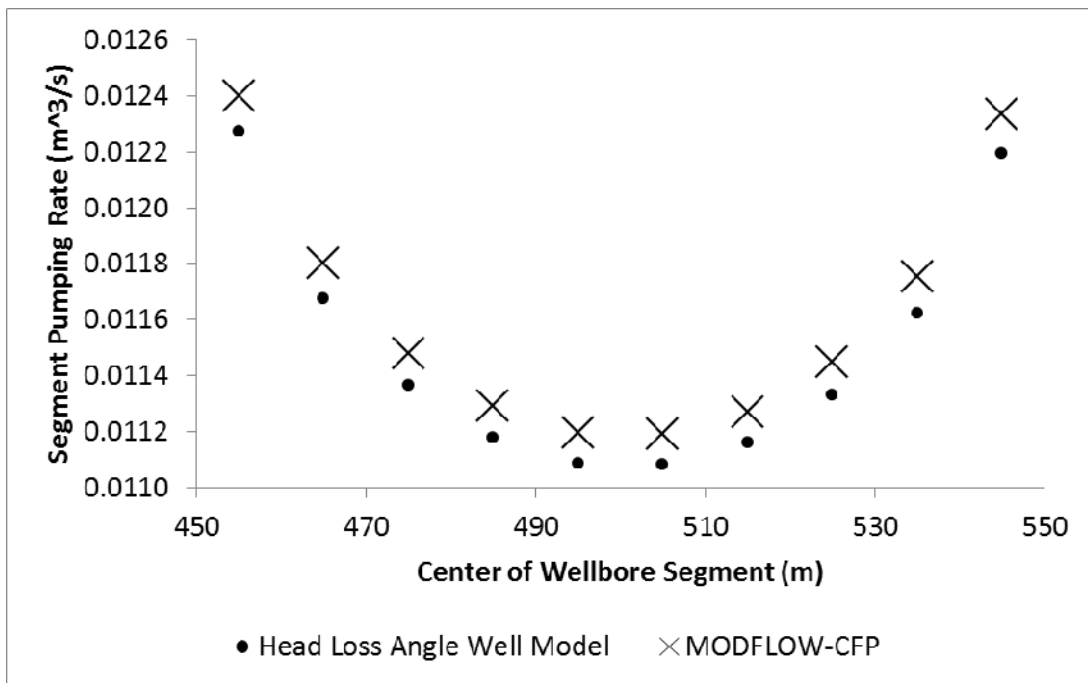


Figure 5. Steady state discharge distribution verification between our model and MODFLOW-CFP.

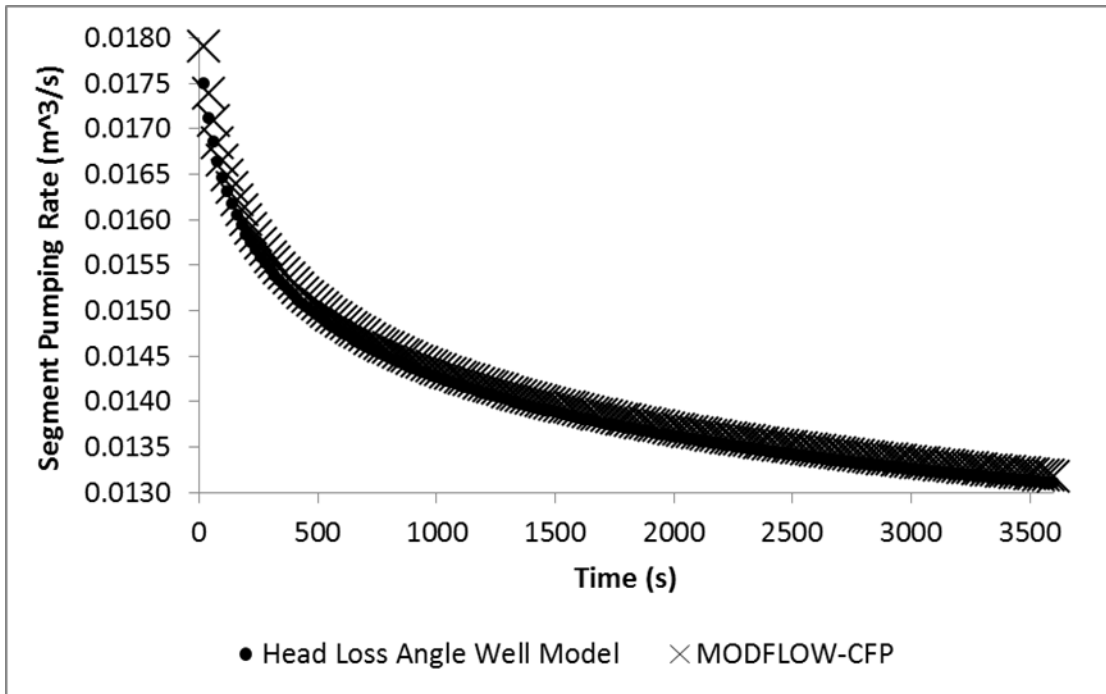


Figure 6. Transient discharge verification of the segment furthest from the constant head segment between our model and MODFLOW-CFP.

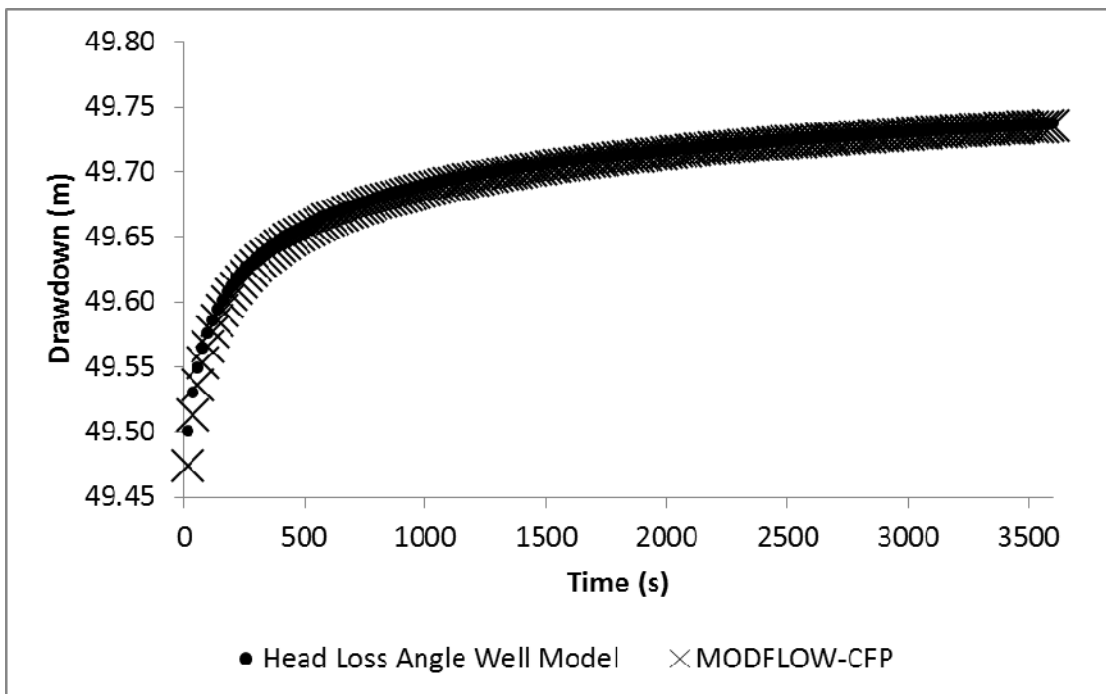


Figure 7. Transient drawdown verification of the segment furthest from the constant head segment between our model and MODFLOW-CFP.

Horizontal Well Cost-Benefit

To investigate well construction limitations, we first derived a new equation for the optimal slant rig entry angle which will minimize the length and therefore cost of a shallow horizontal well. Given a target depth (TVDr) of the lateral section, there is an optimal slant rig angle (angle of the upper section) required to minimize the length of the well. Minimizing the length of the well saves money as less drilling and casing is required. This optimal angle does not consider other factors such as friction, weight on bit or pullback issues. The optimal slant rig entry angle is a function of the target depth and the radius of curvature. If the target is deep, then the optimal entry angle is vertical. However, if the target is shallow – especially if more shallow than the radius of curvature – then optimal slant rig entry angle calculation is necessary.

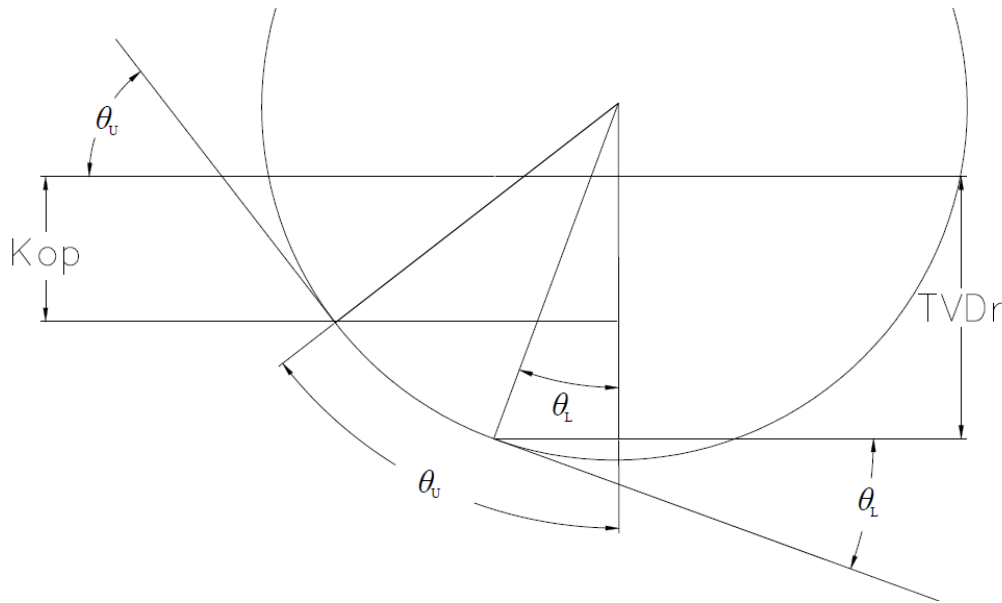


Figure 8. Optimal slant rig entry angle.

To begin derivation, we define the well length as

$$MD = \frac{TVDr - R(\cos[\theta_L] - \cos[\theta_U])}{\sin[\theta_U]} + R(\theta_U - \theta_L) + MD_L,$$

where MD is the measured depth (total length) of the well [L], $TVDr$ is the depth of the upper most part of the lower (horizontal or production) section [L], R is the radius of curvature [L], θ_U is the upper section entry angle, and θ_L is the lower section angle. Using a derivative method to find a solution, the optimal entry angle is

$$\theta_U = \cos^{-1} \left[\cos[\theta_L] - \frac{TVDr}{R} \right] \quad \text{or} \quad \theta_U = \frac{\pi}{2}.$$

We then created a soft string drilling forces model based on petroleum engineering literature (Greenip Jr, 1989; Wu and Juvkam-Wold, 1991). This model calculates required casing and rig strength based on pickup and set down forces (thrust, drag, and torque) for a given well. We then created a cost model based on time and materials. We collected industry well cost data for rigs, directional equipment, cement, and casing. Finally, we combined the optimal entry angle, drilling forces, and well cost models with the collected data to make 60 well cost estimates.

Principal Findings

New Analytical Solutions

In an effort to present new analytical solutions in a concise manner, remember that every three dimensional solution can be subdivided into its three one dimensional components. Thus, the three dimensional solutions take the form

$$d = \int_{t_1}^{t_2} \frac{Q(t-\tau)}{S_s} F_x F_y F_z,$$

where F_x, F_y, F_z are the one dimensional solutions for the $x, y,$ and z directions respectively.

To find the three dimensional solution for a particular time and boundary condition, plug in the appropriate directional components into the following equations and multiply each direction together. Boundary conditions below are written for the x component. For the same BVP solution in another direction, simply replace each directional component element wise. For example, if one wants a solution for the z component replace F_x with F_z, x with z, x_0 with z_0, K_x with K_z, n with $l,$ and a with $c.$

In the following catalog of solutions, the early time (Poisson Re-Summed) equation is presented first and is set equal to the late time (unaltered) equation displayed second. The solution when there is a no-flux boundary at $x = 0$ and $x = a$ is

$$\begin{aligned}
F_x &= \frac{1}{2} \sqrt{\frac{S_s}{\pi K_x \tau}} \sum_{n=-\infty}^{\infty} \left\{ \exp \left[-\frac{S_s (x+x_0+2an)^2}{4\tau K_x} \right] + \exp \left[-\frac{S_s (-x+x_0+2an)^2}{4\tau K_x} \right] \right\} \\
&= \frac{1}{a} \left(1 + 2 \sum_{n=1}^{\infty} \cos \left[\frac{n\pi x}{a} \right] \cos \left[\frac{n\pi x_0}{a} \right] \exp \left[-\tau \frac{n^2 \pi^2 K_x}{a^2 S_s} \right] \right)
\end{aligned}$$

If there is a no flux boundary at $x = 0$ and a constant head boundary at $x = a$, then the solution is

$$\begin{aligned}
F_x &= \frac{1}{2} \sqrt{\frac{S_s}{\pi K_x \tau}} \sum_{n=-\infty}^{\infty} \\
&\quad \left\{ \exp \left[-\frac{S_s (x+x_0+2an)^2}{4\tau K_x} \right] \exp \left[-i \frac{(\pi(x+x_0)/a + 2\pi n)}{2} + i \frac{\pi(x+x_0)}{2a} \right] \right. \\
&\quad \left. + \exp \left[-\frac{S_s (-x+x_0+2an)^2}{4\tau K_x} \right] \exp \left[-i \frac{(\pi(-x+x_0)/a + 2\pi n)}{2} + i \frac{\pi(-x+x_0)}{2a} \right] \right\} \\
&= \frac{2}{a} \sum_{n=0}^{\infty} \cos \left[\frac{(n+1/2)\pi x}{a} \right] \cos \left[\frac{(n+1/2)\pi x_0}{a} \right] \exp \left[-\tau \frac{(n+1/2)^2 \pi^2 K_x}{a^2 S_s} \right]
\end{aligned}$$

If there is a constant head boundary at $x = 0$ and $x = a$, then the solution is

$$\begin{aligned}
F_x &= \frac{1}{2} \sqrt{\frac{S_s}{\pi K_x \tau}} \sum_{n=-\infty}^{\infty} \left\{ \exp \left[-\frac{S_s (-x+x_0+2an)^2}{4\tau K_x} \right] - \exp \left[-\frac{S_s (x+x_0+2an)^2}{4\tau K_x} \right] \right\} \\
&= \frac{2}{a} \sum_{n=1}^{\infty} \sin \left[\frac{n\pi x}{a} \right] \sin \left[\frac{n\pi x_0}{a} \right] \exp \left[-\tau \frac{n^2 \pi^2 K_x}{a^2 S_s} \right]
\end{aligned}$$

Another common boundary condition used in aquifer modeling is the infinite extent condition. In this case we assume that there is a no flux boundary at $x = 0$ and the other reservoir bound at a is infinitely far away. To find a solution when the boundary a is infinitely far away, and there is a no flux boundary at $x = 0$, we take the

$$\lim_{a \rightarrow \infty} \frac{1}{2} \sqrt{\frac{S_s}{\pi K_x \tau}} \sum_{n=-\infty}^{\infty} \left\{ \exp \left[-\frac{S_s (x+x_0+2an)^2}{4\tau K_x} \right] + \exp \left[-\frac{S_s (-x+x_0+2an)^2}{4\tau K_x} \right] \right\},$$

which yields

$$F_x = \frac{1}{2} \sqrt{\frac{S_s}{\pi K_x \tau}} \left(\exp \left[-\frac{S_s (x + x_0)^2}{4\tau K_x} \right] + \exp \left[-\frac{S_s (-x + x_0)^2}{4\tau K_x} \right] \right).$$

It is interesting to note that the solution is in fact the solution for a no-flux boundary using image wells and the assumption of infinite aquifer extents. Similarly, the solution for a constant head boundary at $x = 0$ in an infinite extent aquifer is

$$\lim_{a \rightarrow \infty} \frac{1}{2} \sqrt{\frac{S_s}{\pi K_x \tau}} \sum_{n=-\infty}^{\infty} \left\{ \exp \left[-\frac{S_s (x + x_0 + 2an)^2}{4\tau K_x} \right] - \exp \left[-\frac{S_s (-x + x_0 + 2an)^2}{4\tau K_x} \right] \right\},$$

which yields

$$F_x = \frac{1}{2} \sqrt{\frac{S_s}{\pi K_x \tau}} \left(\exp \left[-\frac{S_s (x + x_0)^2}{4\tau K_x} \right] - \exp \left[-\frac{S_s (-x + x_0)^2}{4\tau K_x} \right] \right).$$

Assuming no boundary conditions, all one needs to do is delete the superimposed image well and the solution takes the form

$$F_x = \frac{1}{2} \sqrt{\frac{S_s}{\pi K_x \tau}} \exp \left[-\frac{S_s (-x + x_0)^2}{4\tau K_x} \right].$$

Intra-Wellbore Head Loss

Using our intra-wellbore head loss model, we completed 360 simulations to investigate intra-wellbore head loss (Figure 9 & 10). We found that only when aquifer drawdown was small will intra-wellbore head loss be relatively important. We found intra-wellbore head loss is relatively important only in extreme scenarios (nearby constant head boundary, high permeability, high pumping rate). We also found that kinetic head loss was greater than friction head loss if the well was less than 10m – 100m long.

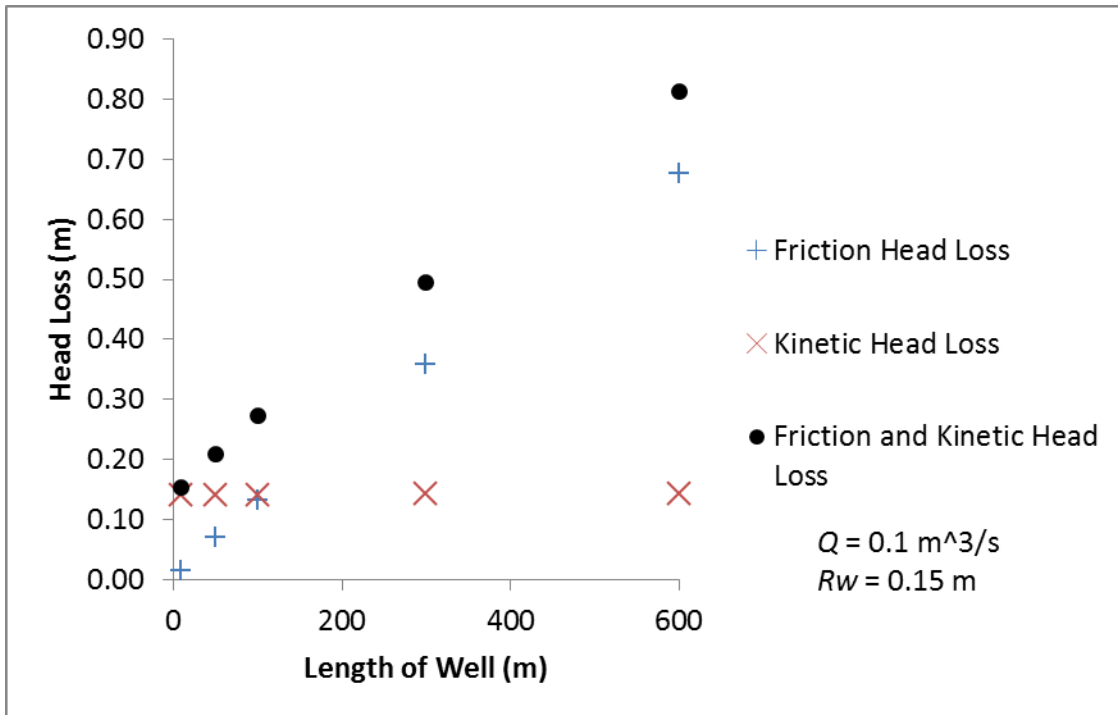


Figure 9. Intra-wellbore head loss.

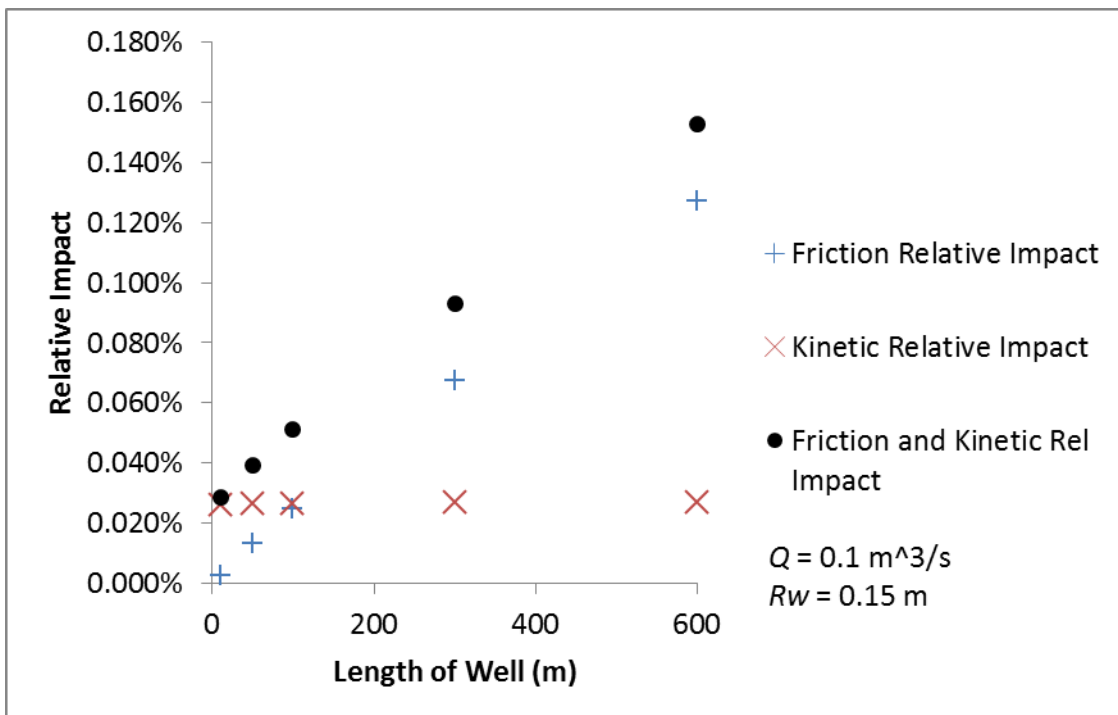


Figure 10. Relative impact of intra-wellbore head loss.

Horizontal Well Cost-Benefit

To investigate well cost, we made cost estimates for 60 wells (Table 1 - Table 4). The most important finding from our cost estimates was that the relative cost of a horizontal well compared to a vertical well decreased with depth. At greater depths a horizontal well is significantly more economically feasible compared to a vertical well (Table 2 & Table 4). We also found that the relative cost between a horizontal well and a vertical well is not dramatically impacted by the rate of penetration. It is interesting, upon comparison of Table 2 & Table 4 that the relative cost of the horizontal well compared to the vertical well is roughly the same (within a factor of two) despite a rate of penetration difference of greater than twenty times.

To investigate horizontal well benefit, we used our aquifer model (Table 5 - Table 8). We found several parameters that increase the number of vertical wells replaced by a horizontal well. These parameters include less time since pumping began, nearby recharge boundaries, vertical fractures, lower permeability, higher specific storativity, and thinner aquifers. Comparing horizontal well benefit with cost, we found that horizontal wells may or may not be economically advantageous depending on site specific conditions.

Table 1. Cost model output assuming rate of penetration is 1,000 ft/day.

ROP = 1,000 ft/day		Length of Horizontal Section (ft)						Rig for Horizontal
		0	500	1,000	1,500	2,000	3,000	
TVD (ft)	50	\$41,964	\$262,460	\$445,236	\$655,567	\$889,743	\$1,429,605	Utility
	250	\$57,186	\$457,806	\$668,705	\$897,803	\$1,145,088	\$1,695,513	Utility
	500	\$103,289	\$763,800	\$1,014,463	\$1,283,325	\$1,570,374	\$2,200,536	Utility
	1,000	\$149,448	\$481,986	\$593,191	\$704,396	\$775,401	\$997,810	Slant Petrol
	1,500	\$200,267	\$520,498	\$637,558	\$725,540	\$845,862	\$1,060,876	Vertical
	2,000	\$243,346	\$635,939	\$740,743	\$853,181	\$959,925	\$1,209,467	Vertical
	3,000	\$385,408	\$968,578	\$1,088,294	\$1,224,021	\$1,346,481	\$1,646,698	Vertical

Table 2. Cost model output assuming rate of penetration is 1,000 ft/day, normalized to vertical well cost.

ROP = 1,000 ft/day		Length of Horizontal Section (ft)						Rig for Horizontal
		0	500	1,000	1,500	2,000	3,000	
TVD (ft)	50	1.0	5.8	9.9	14.5	19.7	31.7	Utility
	250	1.0	8.0	11.7	15.7	20.0	29.6	Utility
	500	1.0	7.4	9.8	12.4	15.2	21.3	Utility
	1,000	1.0	3.2	4.0	4.7	5.2	6.7	Slant Petrol
	1,500	1.0	2.6	3.2	3.6	4.2	5.3	Vertical
	2,000	1.0	2.6	3.0	3.5	3.9	5.0	Vertical
	3,000	1.0	2.5	2.8	3.2	3.5	4.3	Vertical

Table 3. Cost model output assuming rate of penetration is 50 ft/day.

ROP = 50 ft/day		Length of Horizontal Section (ft)						Rig for Horizontal
		0	500	1,000	1,500	2,000	3,000	
TVD (ft)	50	\$41,964	\$262,460	\$445,236	\$655,567	\$889,743	\$1,429,605	Utility
	250	\$88,864	\$457,806	\$668,705	\$897,803	\$1,145,088	\$1,695,513	Utility
	500	\$179,268	\$763,800	\$1,014,463	\$1,283,325	\$1,570,374	\$2,200,536	Utility
	1,000	\$329,705	\$2,733,186	\$3,326,791	\$3,920,396	\$4,514,001	\$5,701,210	Slant Petrol
	1,500	\$502,193	\$2,459,639	\$2,986,529	\$3,536,314	\$4,111,904	\$5,360,300	Vertical
	2,000	\$704,236	\$2,909,282	\$3,483,623	\$4,082,936	\$4,710,447	\$6,072,046	Vertical
	3,000	\$1,252,260	\$4,330,350	\$5,056,038	\$5,814,803	\$6,611,047	\$8,346,189	Vertical

Table 4. Cost model output assuming rate of penetration is 50 ft/day, normalized to vertical well cost.

ROP = 50 ft/day		Length of Horizontal Section (ft)						Rig for Horizontal
		0	500	1,000	1,500	2,000	3,000	
TVD (ft)	50	1.0	5.8	9.9	14.5	19.7	31.7	Utility
	250	1.0	5.2	7.5	10.1	12.9	19.1	Utility
	500	1.0	4.3	5.7	7.2	8.8	12.3	Utility
	1,000	1.0	8.3	10.1	11.9	13.7	17.3	Slant Petrol
	1,500	1.0	4.9	5.9	7.0	8.2	10.7	Vertical
	2,000	1.0	4.1	4.9	5.8	6.7	8.6	Vertical
	3,000	1.0	3.5	4.0	4.6	5.3	6.7	Vertical

Table 5. Vertical well replacement ratios for a gravel aquifer; fifty years.

Aquifer Vertical Thickness (ft)	100	1.00	1.22	1.45	1.57	1.65	1.72	1.77
	90	1.00	1.25	1.47	1.59	1.67	1.73	1.78
	80	1.00	1.29	1.49	1.60	1.68	1.74	1.79
	70	1.00	1.32	1.51	1.62	1.70	1.75	1.80
	60	1.00	1.35	1.53	1.64	1.71	1.77	1.81
	50	1.00	1.38	1.55	1.65	1.72	1.78	1.82
	40	1.00	1.42	1.58	1.67	1.73	1.79	1.83
	30	1.00	1.45	1.60	1.68	1.75	1.80	1.84
	20	1.00	1.48	1.61	1.70	1.76	1.81	1.85
	10	1.00	1.51	1.63	1.71	1.77	1.82	1.86
Gravel	k_x & $k_y = 1E-2$ ft/s $k_z = k_x/10$	0	500	1000	1500	2000	2500	3000
		Horizontal Well Length (ft)						
		$S_s = 1E-5$ /ft, $r_w = 0.5$ ft, end time 50 years, no flux at $z = 0$ & $z = c$, remaining bounds infinitely far away						

Table 6. Vertical well replacement ratios for a silt aquifer; fifty years.

Aquifer Vertical Thickness (ft)	100	1.00	1.42	1.99	2.41	2.76	3.07	3.36
	90	1.00	1.49	2.06	2.48	2.82	3.13	3.42
	80	1.00	1.56	2.13	2.54	2.89	3.20	3.49
	70	1.00	1.64	2.20	2.61	2.95	3.26	3.55
	60	1.00	1.72	2.28	2.68	3.02	3.33	3.61
	50	1.00	1.81	2.36	2.75	3.09	3.39	3.68
	40	1.00	1.91	2.44	2.82	3.16	3.46	3.74
	30	1.00	2.01	2.52	2.89	3.22	3.52	3.88
	20	1.00	2.11	2.59	2.96	3.33	3.62	3.91
	10	1.00	2.20	2.68	3.04	3.36	3.65	3.93
Silt	k_x & $k_y = 1E-7$ ft/s $k_z = k_x/10$	0	500	1000	1500	2000	2500	3000
		Horizontal Well Length (ft)						
		$S_s = 1E-5$ /ft, $r_w = 0.5$ ft, end time 50 years, no flux at $z = 0$ & $z = c$, remaining bounds infinitely far away						

Table 7. Vertical well replacement ratios for a gravel aquifer; one year.

Aquifer Vertical Thickness (ft)	100	1.00	1.27	1.55	1.71	1.83	1.92	2.00
	90	1.00	1.30	1.58	1.74	1.85	1.94	2.02
	80	1.00	1.34	1.61	1.76	1.87	1.96	2.03
	70	1.00	1.38	1.64	1.78	1.89	1.98	2.05
	60	1.00	1.43	1.67	1.81	1.91	1.99	2.06
	50	1.00	1.47	1.69	1.83	1.93	2.01	2.08
	40	1.00	1.51	1.72	1.85	1.95	2.03	2.09
	30	1.00	1.56	1.75	1.87	1.96	2.04	2.11
	20	1.00	1.60	1.78	1.89	1.98	2.05	2.12
	10	1.00	1.63	1.80	1.91	2.00	2.07	2.13
k_x & $k_y = 1E-2$ ft/s $k_z = k_x/10$ Gravel		0	500	1000	1500	2000	2500	3000
		Horizontal Well Length (ft)						
		$S_s = 1E-5$ /ft, $r_w = 0.5$ ft, end time one year, no flux at $z = 0$ & $z = c$, remaining bounds infinitely far away						

Table 8. Vertical well replacement ratios for a silt aquifer; one year.

Aquifer Vertical Thickness (ft)	100	1.00	1.59	2.67	3.71	4.76	5.85	6.96
	90	1.00	1.70	2.83	3.91	5.01	6.15	7.31
	80	1.00	1.82	3.00	4.12	5.27	6.47	7.69
	70	1.00	1.96	3.18	4.36	5.56	6.81	8.10
	60	1.00	2.12	3.39	4.61	5.87	7.18	8.54
	50	1.00	2.30	3.62	4.90	6.22	7.60	9.02
	40	1.00	2.51	3.88	5.22	6.62	8.08	9.60
	30	1.00	2.72	4.11	5.49	6.92	8.44	10.71
	20	1.00	2.96	4.38	5.80	7.59	9.23	11.07
	10	1.00	3.20	4.70	6.20	7.78	9.45	11.19
k_x & $k_y = 1E-7$ ft/s $k_z = k_x/10$ Silt		0	500	1000	1500	2000	2500	3000
		Horizontal Well Length (ft)						
		$S_s = 1E-5$ /ft, $r_w = 0.5$ ft, end time one year, no flux at $z = 0$ & $z = c$, remaining bounds infinitely far away						

Significance

One of the significant contributions of our work is an improved understanding and model of horizontal well drawdown/discharge. This contribution includes new aquifer equations that facilitate a faster, more accurate solution of horizontal well drawdown/discharge. Using these new equations, we have also developed a well model that accounts for intra-wellbore friction and kinetic head loss. Using this model we have determined that intra-wellbore head loss is insignificant for all but extreme cases. We have also determined that kinetic head loss is more significant than friction head loss in shorter wells.

Another significant contribution of our work is a rigorous, deterministic cost-benefit analysis of horizontal wells. In development of this cost-benefit analysis, we also derived an optimal slant rig entry angle equation and models of force (torque, thrust, drag) experienced by the rig and casing. The cost benefit-analysis conducted has revealed that horizontal wells may or may not be economically advantageous depending on site specific conditions. However, we have found several parameters that improve the economics and production benefits of horizontal wells.

References

- Goode, P., 1987. Pressure drawdown and buildup analysis of horizontal wells in anisotropic media. *SPE Formation Evaluation*, 2(4): 683-697.
- Greenip Jr, J.F., 1989. How to design casing strings for horizontal wells. *Petroleum Engineer International*, 61(12).
- Hantush, M., Papadopulos, I., 1962. Flow of ground water to collector wells. *Journal of the Hydraulics Division of the American Society of Civil Engineers*, 88: 221-244.
- Jehn-Dellaport, T., 2004. Innovative water well completion in the Denver Basin, Colorado. *The Mountain Geologist*, 41(4): 211-217.
- Joshi, S.D., 2003. Cost/benefits of horizontal wells, SPE Western Regional/AAPG Pacific Section Joint Meeting. Society of Petroleum Engineers Long Beach, California.
- Odeh, A.S., Babu, D., 1990. Transient flow behavior of horizontal wells, pressure drawdown, and buildup analysis. *SPE Formation evaluation*, 5(1): 7-15.
- Ouyang, L.-B., Arbabi, S., Aziz, K., 1998. General wellbore flow model for horizontal, vertical, and slanted well completions. *SPE Journal*, 3(2): 124-133.
- Park, E., Zhan, H., 2002. Hydraulics of a finite-diameter horizontal well with wellbore storage and skin effect. *Advances in Water Resources*, 25(4): 389-400.
- Penmatcha, V., Aziz, K., 1999. Comprehensive reservoir/wellbore model for horizontal wells. *SPE Journal*, 4(3): 224-234.
- Strikwerda, J.C., 2004. Finite difference schemes and partial differential equations. *Siam*, 435 pp.

Williams, D.E., 2013. Drawdown distribution in the vicinity of nonvertical wells. *Ground Water*, 51(5): 745-751.

Wu, J., Juvkam-Wold, H.C., 1991. Drag and torque calculations for horizontal wells simplified for field use. *Oil & Gas journal*, 89(19): 49-56.

Zhan, H., Wang, L.V., Park, E., 2001. On the horizontal-well pumping tests in anisotropic confined aquifers. *Journal of Hydrology*, 252(1-4): 37-50.

Zhan, H., Zlotnik, V.A., 2002. Groundwater flow to a horizontal or slanted well in an unconfined aquifer. *Water Resources Research*, 38(7): 13-1-13-11.